Demonstration of Neuronal Calcium Sensor-1 binding to the $Ca_V2.1$ P/Q-type calcium channel

Lu-Yun Lian[1*], Sravan R. Pandalaneni[1], Paul A.C. Todd[2], Victoria M. Martin[2], Robert D. Burgoyne[2] and Lee P Haynes[2*].

[1]NMR Centre for Structural Biology, Institute of Integrative Biology, University of Liverpool, Liverpool, UK, L69 3BX

[2]The Physiological Laboratory, Department of Cellular and Molecular Physiology, Institute of Translational Medicine, University of Liverpool, Liverpool, UK, L69 3BX

*Correspondence, L-Y Lian, NMR Centre for Structural Biology, Institute of Integrative Biology, University of Liverpool, Liverpool, UK, L69 3BX, e-mail: lu-yun.lian@liv.ac.uk; LP Haynes, The Physiological Laboratory, Department of Cellular and Molecular Physiology, Institute of Translational Medicine, University of Liverpool, Liverpool, UK, L69 3BX, e-mail: leeh@liv.ac.uk

ABBREVIATIONS

Ca^{2+}, calcium; CaM, Calmodulin; NCS-1, Neuronal Calcium Sensor-1; CaBP, Calcium Binding Protein; Ca_v, Voltage Gated Ca^{2+} Channel; CDI, Ca^{2+} Dependent Inactivation; CDF, Ca^{2+} Dependent Facilitation; CNS, Central Nervous System; PBS, Phosphate Buffered Saline; NTA, Nitrilotriacetic acid; EGTA, Ethylene Glycol Tetraacetic Acid; EDTA, Ethylenediaminetetraacetic acid; SDS, Sodium Dodecyl Sulfate; HEPES, 2-[4-(2-hydroxyethyl)piperazin-1-yl] ethanesulfonic acid; DTT, Dithiothreitol; HRP, Horse Radish Peroxidase; ECL, Enhanced ChemiLuminescence; ITC, Isothermal Titration Calorimetry; NMR, Nuclear Magnetic Resonance; COSY, Correlation Spectroscopy; HSQC, Heteronuclear Single Quantum Correlation;NOESY, Nuclear Overhauser Spectroscopy; TOCSY, Total Correlation Spectroscopy; TOCSY, Total Correlation Spectroscopy.

ABSTRACT

In neurons, entry of extracellular calcium (Ca^{2+}) into synaptic terminals through $Ca_v2.1$ (P/Q-type) Ca^{2+} channels is the driving force for exocytosis of neurotransmitter containing synaptic vesicles. This class of Ca^{2+}-channel is, therefore, pivotal during normal neurotransmission in higher organisms. In response to channel opening and Ca^{2+}-influx, specific Ca^{2+}-binding proteins associate with cytoplasmic regulatory domains of the P/Q-channel to modulate subsequent channel opening. Channel modulation in this way influences synaptic plasticity with consequences for higher level processes such as learning and memory acquisition.

The ubiquitous Ca^{2+}-sensing protein Calmodulin (CaM) regulates the activity of all types of mammalian voltage gated Ca^{2+} channel, including P/Q class, by direct binding to specific regulatory motifs. More recently, experimental evidence has highlighted a role for additional Ca^{2+}-binding proteins, particularly of the CaBP and NCS families in the regulation of P/Q channels. NCS-1 is a protein found from yeast to man and which regulates a diverse number of cellular functions. Physiological and genetic evidence indicates that NCS-1 regulates P/Q channel activity including calcium-dependent facilitation although a direct physical association between the proteins has yet to be demonstrated.

In this study we aimed to determine if there is a direct interaction between NCS-1 and the C-terminal cytoplasmic tail of $Ca_v2.1$ alpha subunit. Using distinct but complimentary approaches including *in vitro* binding of bacterially expressed recombinant proteins, fluorescence spectrophotometry, ITC, NMR and expression of fluorescently tagged proteins in mammalian cells we show direct binding and demonstrate that it can be competed for by CaM. We speculate about how NCS-1/$Ca_v2.1$ association might add to the complexity of calcium channel regulation mediated by other known calcium sensing proteins and how this might help to fine tune neurotransmission in the mammalian central nervous system.

$Ca_v2.1$ P/Q-Type channels are responsible for Ca^{2+} entry into synaptic terminals in many brain regions (*1*). P/Q-type function is therefore pivotal in the regulation of neurotransmitter release and communication throughout the central nervous system (CNS). Indeed, mutations in the gene encoding the human P/Q-α1 subunit are responsible for a number of clinically relevant neurological disorders (*2*). An interesting feature of many Ca_v proteins ($Ca_v1.x$ and $Ca_v2.x$), including the P/Q channel, is that channel activity is itself regulated by Ca^{2+} (*3*). Ca^{2+} dependent channel modulation manifests as two distinct phenomena referred to as Ca^{2+} dependent inactivation (CDI, (*4*)) and Ca^{2+} dependent facilitation (CDF, (*5*)). CDI represents a mechanism by which channels become refractory to further opening in the presence of a sustained stimuli whereas CDF manifests as the opposite process whereby Ca^{2+} augments channel currents (*6*). Specific Ca^{2+}-binding proteins can respond to Ca^{2+} entry through Ca_v channels by interacting directly with regulatory motifs present in the intracellular domains of the α-subunit (*7-10*). These interactions, by currently poorly understood mechanisms, alter channel behaviour to elicit either CDI or CDF. CDI and CDF both have direct impact on synaptic neurotransmitter release, strength of synaptic signalling and ultimately synaptic plasticity. Understanding the basic modes of Ca_v regulation at the molecular level therefore generates insights into more abstract, higher level, processes including learning, memory acquisition, and reasoning.

Of the characterised Ca^{2+}-binding proteins that control Ca_v activity, the ubiquitous small EF-hand containing protein calmodulin (CaM) has been most intensively studied. CaM has been shown to interact with a consensus isoleucine-glutamine 'IQ' motif present in the carboxy terminus of the channel although the precise details of the interaction differs for $Ca_v1.x$ and $Ca_v2.x$ subtypes (*11, 12*). A second Ca^{2+}-dependent CaM binding motif immediately C-terminal to the IQ domain has also been characterised in $Ca_v2.1$ P/Q-type channels (*13*). This CaM Binding Domain (CBD) has been found to influence P/Q channel activity in some studies (*13*) but not others (*7*) and its true significance remains somewhat controversial.

A number of CaM-related Ca^{2+}-binding proteins are enriched in the mammalian CNS and have been found to modulate the properties of Ca_v channels. In all instances thus far characterised, channel regulation is distinct from that observed with CaM suggesting none-redundant functions which have been speculated to permit complex modes of channel regulation and neuronal signalling (*12*). Presently two CaM related Ca^{2+}-binding proteins, Ca^{2+} Binding Protein 1 (CaBP1) and Visinin Like Protein-2 (VILIP-2) have been shown to directly interact with P/Q-Type α-subunits to exert unique regulatory outcomes (*10, 14*). Large numbers of additional CaM-related small EF-hand containing proteins are also expressed in the mammalian CNS. Neuronal Ca^{2+} Sensor-1 (NCS-1) is a CaM-related protein that is evolutionarily conserved from yeast to man (*15*) and that has been implicated in specific human neuronal disorders (*16-19*). Evidence for a regulatory role of NCS-1 on P/Q-Type channels has been reported based on physiological experiments in mammalian cells, including an effect on CDF, (*20-22*) and a genetic study in *Drosophila* (*23*) although no direct interaction between the two proteins has thus far been demonstrated.

In this paper we aimed to use exclusive yet complimentary analytical methods to rigorously determine if there is a direct interaction between NCS-1 and the α-subunit of the P/Q type channel and to provide the first evidence an interaction between a defined region of the C-terminal domain of the P/Q α-subunit and NCS-1. We show that a segment of P/Qα encoding the IQ motif and CBD interacts with NCS-1 in a Ca^{2+} dependent manner. Using mutagenesis and NMR experiments we further refine the NCS-1 binding site to the IQ motif and show that the interaction is competitive with CaM. We provide further evidence using an *ex vivo* HeLa cell model that NCS-1 and the C-terminal tail of $Ca_v2.1$ interact. These novel observations

expand the repertoire of P/Q-Type interacting proteins and add to the potential variety of modes by which such channels can be controlled.

EXPERIMENTAL PROCEDURES

Cloning - DNA constructs and molecular biology – GST-NCS-1 (*24*) and NCS-1-mCherry (*18*) plasmids were as previously described. The coding sequence for human CaM was PCR amplified from oligo $dT_{(15)}$ primed HeLa cell RNA and reverse transcribed first strand cDNA template with the following primer pair (based on Genbank Accession: M19311) containing restriction endonuclease sites (underlined) for sub-cloning into the N-terminal GST tag vector pGex6P-1 (Amersham Biosciences, UK): Sense (*BamHI*) 5'-ATATGGATCCATGGCTGACCAACTGACTG-3'; Antisense (*XhoI*) 5'-ATATCTCGAGTCACTTTGCTGTCATCATTTG-3'. GST-P/Q, encoding residues 1898-2035 of rat P/Q channel-α_1 subunit (Genbank Accession: NM_012918) was PCR amplified from rat brain single strand cDNA template with the following primer pair containing restriction endonuclease sites (underlined) for sub-cloning into pGex6P-1: Sense (*BamHI*) 5'-ATATGGATCCAAGTCCACGGACCTGACAGTG-3'; Antisense (*XhoI*) 5'-ATATCTCGAGCTAGGGGAGGTAGTGTTCGCTGTC-3'. GST-CBD (residues 1950-2035) of rat P/Q channel-α_1 subunit was PCR amplified from the GST-P/Q template using the P/Q reverse primer and the following sense primer containing a *BamHI* site (underlined) for subsequent sub-cloning into pGex6P-1: 5'-ATATGGATCCGAGGGAGGACCCAGCCAAAAC-3'. GST-P/$Q^{IM\rightarrow EE}$ was generated by site directed mutagenesis of GST-P/Q plasmid using Quikchange® reagents and protocol (Agilent Technologies, UK) and the following primer pair: Sense 5'-AAGATCTACGCAGCCATGATGGAGGAGGAGTACTACCGGCAGAGCAAG-3'; Antisense5'-CTTGCTCTGCCGGTAGTACTCCTCCTCCAGCAGGGCTGCGTAGATCTT-3'

SUMO-tagged residues 1909-2035 of the rat P/Q channel-α_1 subunit was PCR amplified from the GST-P/Q template encoding residues 1898-2035 with the following primer pair for sub-cloning into the pOPINS vector: Sense 5`-GCGAACAGATCGGTGGTGCAGCCATGATGATCATGGAG-3`; Antisense 5`-ATGGTCTAGAAAGCTTTAGGGGAGGTAGTGTTCGCTGT-3`. Ligation of the PCR product and *KpnI/HindIII* digested vector employed the infusion reaction method (Clontech) according to the manufacturer's protocol.

Myristoylated PQ (1898-2035, ^{myr}PQ-YFP) was constructed as follows: A DNA fragment encoding the myristoylation sequence taken from (*25*), was inserted between the *XhoI* and *HindIII* sites of pEYFP-N1 (Clontech) to generate p^{myr}EYFP-N1. $PQ^{1898-2035}$ was PCR amplified from the existing pGex template with the following primer pair containing restriction endonuclease sites (underlined) for subsequent sub-cloning into p^{myr}EYFP-N1: Sense (*HindIII*) 5'-ATAT AAG CTT AAG TCC ACG GAC CTG ACA GTG-3'; Antisense (*SacII*) 5'-ATAT CCG CGG GGG GAG GTA GTG TTC GCT GTC-3'. All constructs were verified by dideoxy sequencing (The Sequencing Service, University of Dundee, UK).

Cell culture and plasmid transfections - HeLa cells were cultured in DMEM supplemented with 10% (v/v) foetal bovine serum, 1% (v/v) Penicillin/Streptomyocin and 1% (v/v) non-essential amino acids. All cells were maintained in a humidified atmosphere of 95% air/ 5% CO_2 at 37 °C. Cells were plated onto sterile 13mm round coverslips at a density of $0.25x10^6$ cells/well. After 24 hours, cells were transiently transfected with the indicated expression vectors using GeneJuice transfection reagent (Novagen) according to the manufacturer's

protocol. For single and double transfections 1μg of each plasmid was used.

Cell fixation and confocal imaging analysis - 24 hours post-transfection cells on coverslips were washed with Phosphate Buffered Saline (137mM NaCl, 2.7mM KCl, 10mM Na_2PO_4, 2mM NaH_2PO_4, pH7.4), and then fixed with 4%(v/v) Formaldehyde in PBS for 6 minutes at room temperature. Coverslips were subsequently air-dried and mounted onto microscope slides using Prolong anti-fade glycerol (Life Technologies). Fixed cells were imaged using a Leica TCS-SP2 confocal system (Leica Microsystems, Heidelberg, Germany) with pinhole set to 1 Airy unit and a 63x oil immersion objective with a numerical aperture of 1.3. Images were exported as TIFF files and compiled, processed and analysed with ImageJ and CorelDraw X6 applications.

In vitro Binding Assays - *In vitro* protein binding assays – 5μM of GST-fusion protein (GST-P/Q, GST-P/$Q^{IM\rightarrow EE}$ or GST-CBD) was immobilised on to 30μl glutathione-agarose resin (Thermo Scientific) that had been pre-washed in binding buffer (BB, 150mM KCl, 20mM HEPES (pH7.4), 10%(v/v) Glycerol, 5mM NTA, 5mM EGTA, 1mM DTT, 0.1%(v/v) NP-40) or BB supplemented with 1μM free Ca^{2+} (BB+Ca^{2+}) by incubation for 30min with constant agitation at 4^{o}C. GST-free NCS-1 and CaM were added to samples at 5μM (total final binding assay volumes were 100μl) and incubations continued for 1hr with constant agitation at 4^{o}C. For competition binding assays 5μM GST-P/Q was pre-bound to glutathione-agarose resin in BB+Ca^{2+} by incubation for 30min at 4^{o}C with constant agitation. 5μM NCS-1 was then added to samples in the presence of increasing concentrations of CaM ranging from 0μM to 10μM. Binding reactions were continued for 1hr at 4^{o}C with constant agitation. For the Ca^{2+} dose dependency of the NCS-1/GST-P/Q interaction, 1μM GST-P/Q was incubated with 1μM NCS-1in the presence of increasing concentrations of free Ca^{2+}. For all binding assays glutathione-agarose pellets were collected by centrifugation (3,000rpm, 1min, 4^{o}C), washed three times with 1ml of BB or BB+Ca^{2+} and bound proteins extracted by boiling of final bead pellets for 5min in 50μl of SDS dissociation buffer (125mM HEPES (pH 6.8), 10% (w/v) sucrose, 10% (v/v) glycerol, 4% (w/v) SDS, 1% (v/v) β-mercaptoethanol, 2mM EDTA). Proteins were resolved on 4-12% Tris-Glycine gradient gels (Novex®, Life Technologies, UK) and transferred to nitrocellulose membranes for Western blotting by transverse electrophoresis.

Western Blots - Nitrocellulose filters were blocked by incubation in blocking solution (3% (w/v) skimmed milk powder in PBS) for 1hr at room temperature. Filters were subsequently incubated with primary antibody: rabbit anti-NCS-1 (1:1000 (*26*)) or rabbit anti-Calmodulin (1:500, AbCam, UK) diluted in blocking solution, overnight at 4^{o}C with constant agitation. Filters were washed x3 in PBS supplemented with 0.05% (v/v) Tween-20 (PBST) and twice with PBS before incubation with HRP-conjugated species specific secondary antibody (1:400, anti-Rabbit HRP, Sigma, UK) in blocking solution for 1hr at room temperature. Filters were washed x3 with PBST and twice with PBS prior to application of ECL reagents and visualisation of immunoreactivity using a Chemidoc automated gel/blot documentation system (Biorad, UK). Densitometry analysis of developed Western blots was performed using Quantity-1 software (Biorad, UK). For the Ca^{2+} dose dependency of the NCS-1/GST-P/Q interaction, densitometry data was analysed by applying non-linear curve fitting with OriginPro8 software (OriginLab, MA, USA).

Synthetic Peptide - The peptide used corresponds to residues 1903-1929 of the human P/Q receptor. The synthetic P/Q peptide: TVGKIYAAMMIMEYYRQSKAKKLQAMR

(hereafter referred to as PQIQ peptide) was purchased from GenicBio, China. The peptide was delivered >95% pure.

Protein Expression and Purification - NCS-1 was expressed in E.*coli* strain BL21 (DE3) (Novagen) and purified as previously described (*27*). Expression was induced overnight at 18ºC; cells were harvested, resuspended into lysis buffer (50mM Tris.HCl, pH7.5, 200mM NaCl, 5mM $CaCl_2$, Complete EDTA Free Protease inhibitor (Roche Applied Science)), lysed, centrifuged, filtered and loaded to the Hiprep 16/10 Phenyl FF High Sub (GE Healthcare) column which was pre-equilibrated with Buffer-A (50mM Tris.HCl, pH7.5, 200mM NaCl & 5mM $CaCl_2$). The column was extensively washed with Buffer A, and NCS-1 eluted using MilliQ water. The eluted protein was buffer exchanged into 50mM Tris, pH7.4, 500mM NaCl, the N-terminus his- tag removed by incubating the protein overnight at 4^{o}C using TEV protease (1:20 molar ratio of TEV protease:NCS-1). His-tagged uncleaved NCS-1 and TEV protease were separated for cleaved NCS-1 using a HisTrap FF 5mL affinity column (GE Healthcare). The cleaved NCS-1 was further purified using Superdex 75 Hiload 26/60 (Amersham Biosciences) size exclusion column (50mM TrisHCl, pH7.5, 150mM NaCl). The purity of the sample was assessed by SDS-Page gel and deemed to be >95% pure. Eluted peak was concentrated and stored at -80^{o}C.

Calmodulin was cloned into a pET-15b (Novagen) vector (gift from Dr. Ashraf Kitmitto, University of Manchester) and expressed in E.*coli* strain BL21 (DE3) (Novagen) at 37^{o}C. Harvested cells were resuspended in lysis buffer (50mM Tris (pH 7.5), 2mM DTT), disrupted using the French press (Sim Aminco) at 1000 PSI, centrifuged and the supernatant was recovered, $CaCl_2$ added to a final concentration of 2mM and protein solution loaded onto a 20mL HiPrep^{TM} phenyl sepharose hydrophobic column (GE Healthcare), pre-equilibrated with CaM buffer A (50mM Tris, pH 7.5, 200mM NaCl, 2mM $CaCl_2$, 0.5mM DTT). The column was washed with CaM buffer A, followed by buffer B (50mM Tris, pH 7.5, 0.5mM $CaCl_2$, 0.5mM DTT) and pure calmodulin eluted with CaM buffer C (50mM Tris, pH 7.5, 1mM EGTA, 0.5mM DTT). The protein was further purified using a 26/60 Superdex^{TM} 75 (GE Healthcare) size exclusion column pre-equilibrated with CaM gel filtration (GF) buffer (50mM Tris, pH7.5, 200mM NaCl, 10mM $CaCl_2$, 0.5mM DTT). The sample was loaded before isocratic elution. The purity of the sample was assessed by SDS-PAGE gel and deemed to be >95% pure. CaM was dialysed against water and lyophilised before storage at -20°C.

^{15}-N-labelled SUMO-tagged PQIQ 1909-2035 was expressed in *E. coli* BL21(DE3) in 2M9 medium with overnight incubation 18^{o}C and cells are harvested and resuspended into the lysis buffer (50mM Tris.HCl (pH7.4), 500mM NaCl) supplemented with Compete EDTA Free Protease inhibitor (Roche Applied Science). The cells were lysed, 250µg of bovine pancreas Deoxyribonuclease I (Sigma) added, sample centrifuged and supernatant collected, filtered through 0.22µ acrodisc and loaded onto a HisTrap 5ml FF column (GE Healthcare) pre-equilibrated with buffer A (50 mM Tris.HCl (pH7.4), 500 mM NaCl). Unbound proteins were removed through extensive wash with buffer A, with further successive washes with buffer A containing 10mM, 25mM and 50mM Imidazole. Sumo-tagged PQIQ 1909-2035 was eluted with buffer A containing 250mM imidazole, buffer-exchanged into SUMO cleavage buffer (50mM Tris (pH7.4), 150mM NaCl), SUMO protease was added and solution incubated overnight. Cleaved PQIQ 1909-2035 was separated from the His-SUMO tag by reloading the sample onto the HisTrap 5ml FF column. PQIQ 1909-2035 was further purified using a Superdex 57 26/60 (GE Healthcare) size-exclusion column. The eluted protein was dialysed against Milli Q water and stored as lyophilised samples. Confirmation of the identity of the purified PQIQ 1909-2035 was obtained through MALDI-TOF mass

spectrometry performed on unlabelled PQIQ 1909-2035 prepared using the identical procedure as described above.

Isothermal Titration Calorimetry - ITC experiments were performed using a MicroCal ITC_{200} instrument. Due to limitations in the PQIQ peptide solubility, NCS-1 was titrated into the peptide. Ca^{2+}/NCS-1 at 1mM was prepared by buffer exchange using a PD10 column equilibrated in 50mM Tris (pH7.5), 50mM NaCl, 5mM $CaCl_2$ and the PQIQ peptide solution at 100μM was prepared using the same buffer. If necessary, minor adjustments were made to the pH of the peptide solution. Experiments were carried out using 200μl of 100μM PQIQ peptide in the cell and 60μl of 1mM NCS-1 in the syringe at 25°C. One injection of 0.2μl, followed by 20 injections of 2μl were made with 180sec spacing to allow the baseline to return after each injection. All experiments were performed in triplicate. The data was analysed with a one site (three parameters) curve fitting carried out using the MicroCal-supported ITC module within Origin version 7.

Spectrofluorimetry - To monitor intrinsic tryptophan fluorescence of NCS proteins (*28, 29*), purified recombinant NCS-1 at a concentration of 1μM in a buffer (50mM Tris (pH 7.5), 50mM NaCl, 5mM $CaCl_2$) was excited at room temperature with 280nm wavelength light and emission measured between 290-410nm with a slit width of 20nm using a CARY Eclipse spectrofluorimeter . The PQIQ peptide (stocks ranging from 50μM-1mM) was then added to give an incremental increase in peptide concentration and emission spectra acquired after each addition. Experiments were performed in triplicate. The data for the measured tryptophan fluorescence change at each peptide concentration were fitted to a logistic equation using non-linear curve fitting in OriginPro ™ 9.0.

NMR Spectroscopy - NCS-1 was prepared in Tris buffer (pH 6.8) in the presence of 5mM $CaCl_2$. NMR spectra were recorded at 298K on Bruker Avance II 800 and 600 MHz spectrometers equipped with CryoProbes. Data were processed using the Bruker Software TopSpin and analysed using CCPN software (*30*). Sequence specific assignment of the PQIQ peptide was obtained using homonuclear 2D-TOCSY, COSY and NOESY data. ^{13}C,^{15}N-filtered TOCSY and NOESY experiments were used to assigned the peptide resonances in complex with $^{13}C/^{15}N$ NCS-1.

RESULTS

The aim of this study was to test, using a range of complementary methods, the possibility that the small calcium sensing protein NCS-1 directly interacts with the $Ca_v2.1$ P/Q type Ca^{2+} channel as has been indirectly suggested in prior functional studies (*20-23*). With the knowledge that other known small EF-hand Ca^{2+}-binding proteins interact with the α-subunit of the P/Q channel predominantly through motifs located in the C-terminal tail we reasoned that the same domains represent the most likely sites for an NCS-1 interaction. In initial experiments we generated a recombinant, GST-tagged, form of the P/Q α1 subunit C-terminal tail domain corresponding to residues 1898-2035 (Figure 1, GST-PQ). This fragment encompasses both the IQ motif (IM in the P/Q Type channel) and the CaM binding domain (CBD) (*10*). Two further constructs derived from this precursor were the CBD alone (residues 1950-2035, Figure 1, GST-CBD) and an IQ motif mutant whereby the P/Q-channel IM residues at positions 1913 and 1914 were mutated to glutamic acid to generate an IM→EE double mutant (Figure 1, $GST^{IM\rightarrow EE}$). This mutation has been previously shown to abolish CaM dependent CDF and CDI of the human P/Q-Type channel (*7*). We used these constructs to investigate whether recombinant NCS-1 could associate with P/Q-type C-terminal regulatory domains *in vitro*. NCS-1 exhibited Ca^{2+}-dependent binding to GST-PQ

but was not observed to bind to either GST-CBD or $GST^{IM\rightarrow EE}$ under any tested conditions (Figure 1A) suggesting a specific interaction with residues in the IQ region of the channel.

A Ca^{2+} titration of NCS-1 binding to GST-PQ confirmed the Ca^{2+}-dependency of the interaction and allowed us to derive a K_d of 0.7μM based on densitometry quantification of Western blot data (Figure 1B). For comparison we performed the same binding analysis with CaM (Figure 1C). Similar to our results with NCS-1, CaM displayed Ca^{2+}-dependent binding to GST-PQ but no detectable binding under any conditions to either GST-CBD or $GST^{IM\rightarrow EE}$.

Our initial data suggested that both NCS-1 and CaM could interact with the same IQ-motif region of rat P/Q-Type channel and therefore we extended our binding studies to evaluate the potential existence of a common, overlapping, binding site for both proteins. Competitive association of both proteins with GST-PQ was assessed by binding of NCS-1 to GST-PQ in the presence of increasing concentrations of recombinant CaM (Figure 2). Western blot results from these experiments highlighted a clear displacement of NCS-1 from GST-PQ that was first apparent at a CaM concentration of between 0.3μM and 1μM (Figure 2A). Densitometry analysis of the Western blot data confirmed a competitive association between NCS-1 and CaM for GST-PQ (Figure 2B). Our initial experiments indicated that the IQ like motif of the P/Q-type channel is important for interaction with both NCS-1 and CaM and therefore in subsequent NMR and ITC analyses we focused on this region of the channel only.

Further testing of the ability of NCS-1 to bind the P/Q type channel and to delineate the NCS-1 and CaM binding regions of the P/Q-type channel was performed using NMR experiments. A sample of ^{15}N-labelled P/Q spanning residues 1909 to 2035 (encompassing much of the IQ motif and the CBD) was prepared. Addition of CaM shows chemical shift perturbations of glycine and tryptophan residues whereas NCS-1 has no effect on either group of residues (Figure 3). Glycine and tryptophan residues are located in the CBD region but not in or around the IQ segment. Hence, it is clear that NCS-1 does not bind to the CBD of the P/Q channel, although there is indication that there is weak CaM binding to this site.

Knowing from the experiments above that the major site of binding of NCS-1 on the P/Q C-terminal domain was likely to be the IQ motif, further experiments used a synthetic PQIQ peptide. The intrinsic tryptophan fluorescence of NCS-1 was used to measure interactions with the PQIQ peptide, using a smilar approach to that described for the interactions with the D2 dopamine receptor peptide(*27*). NCS-1 has two tryptophan residues; addition of the PQIQ peptide resulted in a decrease in fluorescence and allowed titration of the peptide over a range of concentrations (Figure 2A). The data for the change in fluorescence versus concentration was analysed using a logistic fit. The dose-response upon titration with the PQIQ indicated half-maximal binding at 1.036±_0.07μM with a Hill coefficient of 1.7. Hill coefficients greater than 1 would be consistent with a 2:1 stoichiometry of peptide binding to NCS-1 since NCS-1 itself was monomeric(*27*). Isothermal titration calorimetry (ITC) shows that the interaction is entropically-driven. Due to tendency of the protein complex to aggregate at the high peptide (100μM) and protein concentrations (1mM) required to observed binding by this method, it was not possible to obtain reliable equilibrium binding constants using ITC. The affinity obtained for NCS-1 interaction with the PQIQ peptide is almost an order of magnitude lower than the reported affinities involving the calmodulin lobes; From ITC experiments, K_d values of 51±20nM and 4.32±0.39nM were obtained, for, respectively, the Ca^{2+}/N and Ca^{2+}/C lobe binding to the IQ domain of the PQ channel (*31*). The two lobes in NCS-1 are intimately linked and attempts to express the two NCS-1 lobes as independently folded domains soluble at micomolar concentrations have been met with little success so far.

Therefore, experiments to disentangle the relatively affinities of the two NCS-1 domains for the PQIQ peptide have not been possible.

To determine which region of the PQIQ peptide forms the NCS-1 binding site we again used NMR. In these experiments $^{13}C/^{15}N$- NCS-1 was titrated into a sample of the unlabelled PQIQ peptide and$^{13}C/^{15}N$ filtered TOCSY and NOESY data acquired. Analysis of the side-chain resonances, in particular the methyl and tyrosine resonances, reveal selective line-broadening for fourteen residues, YAAMMIMEYYRQSK (Figure 5A). Hence, a subset of the 27 amino acids in the polypeptide sequence forms the main interaction site for NCS-1 binding, with the residues beyond this core peptide region further enhancing the interaction. The length of this motif correlates well with the recently reported structure of NCS-1 in complex with the C-terminus peptide from the human D2 dopamine receptor (PDB Accession 2YOU). The 14 amino acid motif is short enough for it to bind NCS-1 with a stoichiometry of 2:1 (peptide:NCS-1) and supports the fluorescence binding data.

NMR $^{1}H-^{15}N$ HSQC of NCS-1 in the presence of two-fold excess of PQIQ show resonances which are universally broadened although still discernable to confirm that the protein remains folded (Figure 5B). Addition of equimolar amounts of unlabelled CaM/Ca^{2+} to the preformed ^{15}N-labelled NCS-1/PQIQ complex led to a complete reversion of the $^{1}H-^{15}N$ HSQC C spectrum to that of free NCS-1. This is further confirmation that NCS-1 and CaM bind to the similar sites on the PQ channel, with, as expected, CaM binding the peptide strong enough to displace it from NCS-1.

The experiments described above show that a direct interaction of NCS-1 with the P/Q C-terminus could be detected using three distinct *in vitro* biochemical approaches. In order to provide evidence for the interaction of NCS-1 with the P/Q channel regulatory domain in a more physiological setting the localisation of these proteins was studied *ex vivo* in cultured HeLa cells. For these experiments we returned to the use of a longer recombinant construct encompassing both the IQ and CBD domains of the P/Q C-terminus. We firstly examined the cellular localisation of both NCS-1-mCherry (*18*) and a C-terminally YFP tagged variant of P/Q 1898-2035 to which an N-terminal myristoylation consensus sequence had been attached (^{myr}PQ-YFP). In previous studies this approach has been used to successfully direct isolated soluble domains of plasma membrane proteins to the plasma membrane for functional analyses (*25*). NCS-1-mCherry exhibited a predominantly peri-nuclear localisation consistent with its association with the TGN in addition to some plasma membrane localisation (Figure 6A) (*32*). ^{myr}PQ-YFP was observed to target to the plasma membrane and/or to large cytosolic puncta (Figure 6A). Plasma membrane association of ^{myr}PQ-YFP suggested that myristoylation of the peptide was accurately targeting a fraction of PQ to the expected location. Interestingly, in cells exhibiting ^{myr}PQ-YFP puncta, co-expressed NCS-1-mCherry failed to localise to the TGN or plasma membrane and instead co-localised with ^{myr}PQ-YFP on the enlarged punctate structures (Figure 6B). We quantified these phenomena and were able to demonstrate that in 39.5% ± 9.2% of cells co-transfected with NCS-1-mCherry and ^{myr}PQ-YFP, puncta were observed and that in 100% of this sub-population NCS-1 protein was associated with large ^{myr}PQ-YFP positive punctate structures (Figure 6C, NCS-1-mCh + ^{myr}PQ-YFP). This was similar to the number of cells exhibiting puncta in ^{myr}PQ-YFP/mCherry controls (43.6% ± 3%, Figure 6C, ^{myr}PQ-YFP + mCherry). In contrast, control cells expressing NCS-1-mCherry along with EYFP protein exhibited no observable puncta formation (Figure 6C, NCS-1-mCh + EYFP). It should be noted that co-localisation of NCS-1-mCherry with ^{myr}PQ-YFP in punctate structures was specific for NCS-1 as no co-localisation was observed with the soluble mCherry protein in control co-transfections (data

not shown). These observations are consistent with a direct interaction of NCS-1-mCherry with ^{myr}PQ-YFP in a cellular context.

DISCUSSION

In this paper we set out to examine whether NCS-1 is able to interact directly with the C-terminus of the α1 subunit of P/Q-type channel. To avoid a potentially misleading indication of a positive interaction we tested this using three separate *in vitro* biochemical/biophysical assays using either a long construct from the P/Q C-terminus or a synthetic IQ domain peptide as well as a test through cellular co-localisation. The use of multiple techniques gives a more rigorous approach to addressing the question of whether a significant direct interaction does exist. In all cases we were able to detect a direct interaction between NCS-1 and P/Q-type Ca^{2+}-channels.

P/Q-type channel regulation by small Ca^{2+}-binding proteins is essential in the mammalian CNS for the processes of CDI and CDF which drive short-term pre-synaptic plasticity (*6*). Alterations in synaptic plasticity of this form in turn influence information processing and neural network behaviour which underpin normal functioning of the CNS (*33*). A large body of experimental evidence has been accrued that describes at the molecular level how CaM is able to regulate all Ca_v-type channels including those of the P/Q-subtype. CaM is constitutively associated with P/Qα and is considered an auxiliary subunit of the channel. Apo-CaM is believed to bind to P/Qα at a site outside of, but in close proximity to, the Ca^{2+}-dependent IQ binding site, as determined using a Förster Resonance Energy Transfer approach in cultured mammalian cells (*34*). It has been speculated that this arrangement locates CaM within striking distance of the regulatory IQ motif to ensure fast responses to Ca^{2+} influx on channel opening (*34*). Ca^{2+}-dependent binding of CaM to the IQ motif is then able to modulate both CDI and CDF depending on the precise nature of the Ca^{2+} signal. Mechanistically this system has been resolved in elegant experiments showing that Ca^{2+} entry through individual P/Qα channels selectively activates the CaM C-lobe to mediate CDF. Larger Ca^{2+} signals emanating from multiple local channel opening events conversely activates the CaM N-lobe to drive CDI (*3, 7, 35*). Our data confirming a Ca^{2+}-dependent interaction of CaM with the P/Q-IQ containing motif is consistent with previous biochemical (*7*) and structural analyses (*31*). A second CaM binding site, the CaM-Binding Domain or CBD, has been reported in related studies of P/Q-channel interactions (*5, 13*). In this study, although we have been unable to replicate binding of CaM to this region of the rat α_{1A} CBD using pull-down experiments, the NMR data suggests that CaM, but not NCS-1, binds to the proposed CBD, albeit rather weakly. The weak nature of this interaction might explain why there are discrepancies in the literature regarding the significance of the CBD. Pull-down type experiments select for high-affinity interactions whereas NMR approaches are able to detect lower affinity transient binding events consistent with these results. Our data help reconcile apparently conflicting experimental data whereby some studies do observe a CaM-CBD interaction (*5, 13*) whereas others do not (*7*).

NCS-1, a multifunctional Ca^{2+}-sensor conserved from yeast to man, has documented roles in the regulation of membrane trafficking (*36, 37*), ion channel activity (*38, 39*), dopamine receptor signalling (*27, 40*), Long Term Depression (*41*), autism (*18, 42*) and memory acquisition (*43, 44*). NCS-1 exhibits enriched expression in mammalian brain tissue (*45*) and many of the aforementioned functions are related to neuronal activity. NCS-1 interacts with a number of targets in common with CaM (*24*) and a previous functional study identified links between NCS-1 and CDF of P/Q-Type channel activity in rat primary neurons (*20*). Other studies have additionally indicated a cellular connection between NCS-1 and P/Q-Type

channel activity in bovine adrenal chromaffin cells (*21, 22*) and *Drosophila* (*23*). With this information in mind we have tested the possibility that NCS-1 can directly bind to P/Q regulatory elements in common with CaM and other EF-hand containing Ca^{2+}-sensors (*10, 14*). Our data show that NCS-1 can associate with the IQ motif of rat P/Qα_{1A} in a Ca^{2+}-dependent manner and that this binding site must overlap to some extent with that of CaM since CaM can compete for binding to the same region leading to NCS-1 displacement. This is the first example of a CaM-related Ca^{2+}-sensing protein behaving in an almost identical manner to CaM with respect to IQ binding. Both CaBP1 (*10*) and VILIP-2 (*14*) interact with the CBD or require this domain for functional activity. CaM binds predominantly to the IQ domain with a possible weak interaction with the CBD, and NCS-1 binds only to the IQ domain in the presence of Ca^{2+}. The weak CaM-CBD interaction that we have observed in this study might also help to explain why CaBP1 and VILIP-2 are able to effectively compete with CaM at this site (*10, 14*).

The precise details of the NCS-1 interaction are still to be elucidated. In rat primary neurons NCS-1 appears to play a role during CDF (*20*) and in *Drosophila*, loss of the NCS-1 orthologue Frequenin leads to reduced Ca^{2+} entry into neurons and defective synaptic transmission (*23*). These data suggest that at least one function of NCS-1 is in positively regulating P/Q channel opening. Our data now provide an attractive biochemical explanation for these cellular studies and act as a platform for further cellular and structural investigations studying the interplay between CaM and NCS-1 during regulation of P/Q channel activity. CaM is expressed in all neurons and one possibility is that specific neuronal populations that also express NCS-1 are able to utilise this Ca^{2+}-sensor as an additional modulator of P/Q activity. NCS-1 has a higher Ca^{2+} affinity than CaM (*15, 46*) and therefore could potentially interact with the IQ motif over a different range of local Ca^{2+}-concentrations to modulate activity independently of CaM. As Ca^{2+} concentrations increase CaM could then displace NCS-1 to exert its documented roles in CDF and CDI. The N- and C-lobes of CaM, as described, exert distinct modes of P/Q-channel regulation. NCS-1, unlike CaM, does not have distinct lobes but rather a compact globular structure (*47*). The orientations of the N and C lobes with respect to one another differ in the two proteins, giving rise to different conformations of the ligand-binding site. Residues from both lobes in NCS-1 together form a large, contiguous solvent exposed hydrophobic ligand-binding crevice, resembling the palm of a partially-open hand. In Ca^{2+}/CaM-PQIQ complex, the hydrophobic binding pocket is more enclosed, resembling a closed hand which envelopes the PQIQ peptide. It is, therefore, not possible to model a structure of NCS-1 in complex with the PQIQ peptide based on the Ca^{2+}/CaM complex structure. It is likely that binding the PQIQ peptide would require a significant conformational change to the overall structure of NCS-1 in order to accommodate the peptide.

Using a combination of *in vitro* biochemical, NMR/ITC biophysical and cellular approaches we provide the first evidence for a direct interaction of NCS-1 with P/Q-Type voltage gated Ca^{2+} channels. Voltage gated Ca^{2+} channel modulation has direct implications for synaptic plasticity and complex neural processing in higher organisms. Our work expands the number of small Ca^{2+}-sensing proteins able to interact with the essential P/Q-type neuronal channel and provides further insights into the complexity in regulation of voltage gated Ca^{2+} channels in the mammalian CNS. Extensive further work will be required to determine the full structural basis for the interaction of NCS-1 with the P/Q IQ domain.

ACKNOWLEDGEMENTS

This work was supported by Wellcome Trust Prize PhD studentships awarded to V.M.M and P.A.C.T, and a University of Liverpool Studentship awarded to S.R.P.

REFERENCES

1. Olivera, B. M., Miljanich, G. P., Ramachandran, J., and Adams, M. E. (1994) Calcium channel diversity and neurotransmitter release: the omega-conotoxins and omega-agatoxins, *Annu Rev Biochem 63*, 823-867.
2. Rajakulendran, S., Kaski, D., and Hanna, M. G. (2012) Neuronal P/Q-type calcium channel dysfunction in inherited disorders of the CNS, *Nature reviews. Neurology 8*, 86-96.
3. Liang, H., DeMaria, C. D., Erickson, M. G., Mori, M. X., Alseikhan, B. A., and Yue, D. T. (2003) Unified mechanisms of Ca2+ regulation across the Ca2+ channel family, *Neuron 39*, 951-960.
4. Budde, T., Meuth, S., and Pape, H. C. (2002) Calcium-dependent inactivation of neuronal calcium channels, *Nat Rev Neurosci 3*, 873-883.
5. Lee, A., Scheuer, T., and Catterall, W. A. (2000) Ca2+/calmodulin-dependent facilitation and inactivation of P/Q-type Ca2+ channels, *J Neurosci 20*, 6830-6838.
6. Catterall, W. A., and Few, A. P. (2008) Calcium channel regulation and presynaptic plasticity, *Neuron 59*, 882-901.
7. DeMaria, C. D., Soong, T. W., Alseikhan, B. A., Alvania, R. S., and Yue, D. T. (2001) Calmodulin bifurcates the local Ca2+ signal that modulates P/Q-type Ca2+ channels, *Nature 411*, 484-489.
8. Lee, A., Zhou, H., Scheuer, T., and Catterall, W. A. (2003) Molecular determinants of Ca(2+)/calmodulin-dependent regulation of Ca(v)2.1 channels, *Proc Natl Acad Sci U S A 100*, 16059-16064.
9. Findeisen, F., and Minor, D. L., Jr. (2010) Structural basis for the differential effects of CaBP1 and calmodulin on Ca(V)1.2 calcium-dependent inactivation, *Structure 18*, 1617-1631.
10. Lee, A., Westenbroek, R. E., Haeseleer, F., Palczewski, K., Scheuer, T., and Catterall, W. A. (2002) Differential modulation of Ca(v)2.1 channels by calmodulin and Ca2+-binding protein 1, *Nat Neurosci 5*, 210-217.
11. Pate, P., Mochca-Morales, J., Wu, Y., Zhang, J. Z., Rodney, G. G., Serysheva, II, Williams, B. Y., Anderson, M. E., and Hamilton, S. L. (2000) Determinants for calmodulin binding on voltage-dependent Ca2+ channels, *J Biol Chem 275*, 39786-39792.
12. Minor, D. L., Jr., and Findeisen, F. (2010) Progress in the structural understanding of voltage-gated calcium channel (CaV) function and modulation, *Channels (Austin) 4*, 459-474.
13. Lee, A., Wong, S. T., Gallagher, D., Li, B., Storm, D. R., Scheuer, T., and Catterall, W. A. (1999) Ca2+/calmodulin binds to and modulates P/Q-type calcium channels, *Nature 399*, 155-159.
14. Lautermilch, N. J., Few, A. P., Scheuer, T., and Catterall, W. A. (2005) Modulation of CaV2.1 channels by the neuronal calcium-binding protein visinin-like protein-2, *J Neurosci 25*, 7062-7070.
15. Burgoyne, R. D., and Weiss, J. L. (2001) The neuronal calcium sensor family of Ca2+-binding proteins, *Biochem J 353*, 1-12.
16. Weiss, J. L., Hui, H., and Burgoyne, R. D. (2010) Neuronal calcium sensor-1 regulation of calcium channels, secretion, and neuronal outgrowth, *Cell Mol Neurobiol 30*, 1283-1292.
17. Dason, J. S., Romero-Pozuelo, J., Atwood, H. L., and Ferrus, A. (2012) Multiple roles for frequenin/NCS-1 in synaptic function and development, *Mol Neurobiol 45*, 388-402.

18. Handley, M. T., Lian, L. Y., Haynes, L. P., and Burgoyne, R. D. (2010) Structural and functional deficits in a neuronal calcium sensor-1 mutant identified in a case of autistic spectrum disorder, *PLoS One 5*, e10534.
19. Pavlowsky, A., Gianfelice, A., Pallotto, M., Zanchi, A., Vara, H., Khelfaoui, M., Valnegri, P., Rezai, X., Bassani, S., Brambilla, D., Kumpost, J., Blahos, J., Roux, M. J., Humeau, Y., Chelly, J., Passafaro, M., Giustetto, M., Billuart, P., and Sala, C. (2010) A postsynaptic signaling pathway that may account for the cognitive defect due to IL1RAPL1 mutation, *Curr Biol 20*, 103-115.
20. Tsujimoto, T., Jeromin, A., Saitoh, N., Roder, J. C., and Takahashi, T. (2002) Neuronal calcium sensor 1 and activity-dependent facilitation of P/Q-type calcium currents at presynaptic nerve terminals, *Science 295*, 2276-2279.
21. Weiss, J. L., Archer, D. A., and Burgoyne, R. D. (2000) Neuronal Ca2+ sensor-1/frequenin functions in an autocrine pathway regulating Ca2+ channels in bovine adrenal chromaffin cells, *J Biol Chem 275*, 40082-40087.
22. Weiss, J. L., and Burgoyne, R. D. (2001) Voltage-independent inhibition of P/Q-type Ca2+ channels in adrenal chromaffin cells via a neuronal Ca2+ sensor-1-dependent pathway involves Src family tyrosine kinase, *J Biol Chem 276*, 44804-44811.
23. Dason, J. S., Romero-Pozuelo, J., Marin, L., Iyengar, B. G., Klose, M. K., Ferrus, A., and Atwood, H. L. (2009) Frequenin/NCS-1 and the Ca2+-channel alpha1-subunit co-regulate synaptic transmission and nerve-terminal growth, *J Cell Sci 122*, 4109-4121.
24. Haynes, L. P., Fitzgerald, D. J., Wareing, B., O'Callaghan, D. W., Morgan, A., and Burgoyne, R. D. (2006) Analysis of the interacting partners of the neuronal calcium-binding proteins L-CaBP1, hippocalcin, NCS-1 and neurocalcin delta, *Proteomics 6*, 1822-1832.
25. Oz, S., Benmocha, A., Sasson, Y., Sachyani, D., Almagor, L., Lee, A., Hirsch, J. A., and Dascal, N. (2013) Competitive and non-competitive regulation of calcium-dependent inactivation in CaV1.2 L-type Ca2+ channels by calmodulin and Ca2+-binding protein 1, *J Biol Chem 288*, 12680-12691.
26. McFerran, B. W., Graham, M. E., and Burgoyne, R. D. (1998) Neuronal Ca2+ sensor 1, the mammalian homologue of frequenin, is expressed in chromaffin and PC12 cells and regulates neurosecretion from dense-core granules, *J Biol Chem 273*, 22768-22772.
27. Lian, L. Y., Pandalaneni, S. R., Patel, P., McCue, H. V., Haynes, L. P., and Burgoyne, R. D. (2011) Characterisation of the interaction of the C-terminus of the dopamine d2 receptor with neuronal calcium sensor-1, *PLoS One 6*, e27779.
28. McFerran, B. W., Weiss, J. L., and Burgoyne, R. D. (1999) Neuronal Ca(2+) sensor 1. Characterization of the myristoylated protein, its cellular effects in permeabilized adrenal chromaffin cells, Ca(2+)-independent membrane association, and interaction with binding proteins, suggesting a role in rapid Ca(2+) signal transduction, *J Biol Chem 274*, 30258-30265.
29. Haynes, L. P., Tepikin, A. V., and Burgoyne, R. D. (2004) Calcium-binding protein 1 is an inhibitor of agonist-evoked, inositol 1,4,5-trisphosphate-mediated calcium signaling, *J Biol Chem 279*, 547-555.
30. Vranken, W. F., Boucher, W., Stevens, T. J., Fogh, R. H., Pajon, A., Llinas, M., Ulrich, E. L., Markley, J. L., Ionides, J., and Laue, E. D. (2005) The CCPN data model for NMR spectroscopy: development of a software pipeline, *Proteins 59*, 687-696.
31. Kim, E. Y., Rumpf, C. H., Fujiwara, Y., Cooley, E. S., Van Petegem, F., and Minor, D. L., Jr. (2008) Structures of CaV2 Ca2+/CaM-IQ domain complexes reveal binding

modes that underlie calcium-dependent inactivation and facilitation, *Structure 16*, 1455-1467.
32. Haynes, L. P., Sherwood, M. W., Dolman, N. J., and Burgoyne, R. D. (2007) Specificity, promiscuity and localization of ARF protein interactions with NCS-1 and phosphatidylinositol-4 kinase-III beta, *Traffic 8*, 1080-1092.
33. Abbott, L. F., and Regehr, W. G. (2004) Synaptic computation, *Nature 431*, 796-803.
34. Erickson, M. G., Alseikhan, B. A., Peterson, B. Z., and Yue, D. T. (2001) Preassociation of calmodulin with voltage-gated Ca(2+) channels revealed by FRET in single living cells, *Neuron 31*, 973-985.
35. Park, H. Y., Kim, S. A., Korlach, J., Rhoades, E., Kwok, L. W., Zipfel, W. R., Waxham, M. N., Webb, W. W., and Pollack, L. (2008) Conformational changes of calmodulin upon Ca2+ binding studied with a microfluidic mixer, *Proc Natl Acad Sci U S A 105*, 542-547.
36. Zhao, X., Varnai, P., Tuymetova, G., Balla, A., Toth, Z. E., Oker-Blom, C., Roder, J., Jeromin, A., and Balla, T. (2001) Interaction of neuronal calcium sensor-1 (NCS-1) with phosphatidylinositol 4-kinase beta stimulates lipid kinase activity and affects membrane trafficking in COS-7 cells, *J Biol Chem 276*, 40183-40189.
37. Haynes, L. P., Thomas, G. M., and Burgoyne, R. D. (2005) Interaction of neuronal calcium sensor-1 and ADP-ribosylation factor 1 allows bidirectional control of phosphatidylinositol 4-kinase beta and trans-Golgi network-plasma membrane traffic, *J Biol Chem 280*, 6047-6054.
38. Hui, H., McHugh, D., Hannan, M., Zeng, F., Xu, S. Z., Khan, S. U., Levenson, R., Beech, D. J., and Weiss, J. L. (2006) Calcium-sensing mechanism in TRPC5 channels contributing to retardation of neurite outgrowth, *J Physiol 572*, 165-172.
39. Guo, W., Malin, S. A., Johns, D. C., Jeromin, A., and Nerbonne, J. M. (2002) Modulation of Kv4-encoded K(+) currents in the mammalian myocardium by neuronal calcium sensor-1, *J Biol Chem 277*, 26436-26443.
40. Kabbani, N., Negyessy, L., Lin, R., Goldman-Rakic, P., and Levenson, R. (2002) Interaction with neuronal calcium sensor NCS-1 mediates desensitization of the D2 dopamine receptor, *J Neurosci 22*, 8476-8486.
41. Jo, J., Heon, S., Kim, M. J., Son, G. H., Park, Y., Henley, J. M., Weiss, J. L., Sheng, M., Collingridge, G. L., and Cho, K. (2008) Metabotropic glutamate receptor-mediated LTD involves two interacting Ca(2+) sensors, NCS-1 and PICK1, *Neuron 60*, 1095-1111.
42. Piton, A., Michaud, J. L., Peng, H., Aradhya, S., Gauthier, J., Mottron, L., Champagne, N., Lafreniere, R. G., Hamdan, F. F., team, S. D., Joober, R., Fombonne, E., Marineau, C., Cossette, P., Dube, M. P., Haghighi, P., Drapeau, P., Barker, P. A., Carbonetto, S., and Rouleau, G. A. (2008) Mutations in the calcium-related gene IL1RAPL1 are associated with autism, *Hum Mol Genet 17*, 3965-3974.
43. Gomez, M., De Castro, E., Guarin, E., Sasakura, H., Kuhara, A., Mori, I., Bartfai, T., Bargmann, C. I., and Nef, P. (2001) Ca2+ signaling via the neuronal calcium sensor-1 regulates associative learning and memory in C. elegans, *Neuron 30*, 241-248.
44. Saab, B. J., Georgiou, J., Nath, A., Lee, F. J., Wang, M., Michalon, A., Liu, F., Mansuy, I. M., and Roder, J. C. (2009) NCS-1 in the dentate gyrus promotes exploration, synaptic plasticity, and rapid acquisition of spatial memory, *Neuron 63*, 643-656.
45. Paterlini, M., Revilla, V., Grant, A. L., and Wisden, W. (2000) Expression of the neuronal calcium sensor protein family in the rat brain, *Neuroscience 99*, 205-216.
46. Burgoyne, R. D. (2007) Neuronal calcium sensor proteins: generating diversity in neuronal Ca2+ signalling, *Nat Rev Neurosci 8*, 182-193.

47. Bourne, Y., Dannenberg, J., Pollmann, V., Marchot, P., and Pongs, O. (2001) Immunocytochemical localization and crystal structure of human frequenin (neuronal calcium sensor 1), *J Biol Chem 276*, 11949-11955.

FIGURE LEGENDS

FIGURE 1 – *NCS-1 and CaM interactions with rat PQα_1-subunit C-terminal binding motifs*. A) Recombinant NCS-1 was incubated with GST-PQ (residues 1898-2035 of rat PQα_1 subunit, encompassing both the IQ and CBD motifs), $GST^{IM\rightarrow EE}$ (equivalent to the IQ motif present in $Ca_v1.x$ channels) and GST-CBD (residues 1950-2035 of rat PQα_1 subunit) in the presence or absence of 1μM free Ca^{2+}. Bound NCS-1 was detected by Western blotting with a specific antibody. This blot is a representative result and averaged data from 3 independent binding assays is presented in Supplementary Table 1. B) Densitometry quantification of an NCS-1/GST-PQ binding Ca^{2+} dose response. Recombinant NCS-1 (1μM) was incubated with 1μM GST-PQ in the presence of increasing concentrations of free Ca^{2+} and bound protein detected by Western blotting with anti-NCS-1 specific antibody. Western blot signal intensities were quantified by densitometry and plotted as a function of the free Ca^{2+} concentration present in the binding reaction. C) Recombinant CaM was incubated with GST-PQ, $GST^{IM\rightarrow EE}$ and GST-CBD in the presence or absence of 1μM free Ca^{2+}. Bound CaM was detected by Western blotting with a specific antibody.

FIGURE 2 – *Competitive interaction between NCS-1 and CaM for binding to GST-PQ*. A) 5μM NCS-1 was incubated with 5 μM GST-PQ in the presence of varying concentrations of CaM. Bound NCS-1 and CaM were visualised by Western blotting with specific antibodies. B) Data from (A) was quantified by densitometry and NCS-1/CaM bound to GST-PQ plotted as a function of the CaM concentration present in the binding assay.

FIGURE 3 - *Delineation of NCS-1 binding to PQ1909-2035*. ^{1}H-^{15}N HSQC spectra of ^{15}N-labelled PQ1909-2035 in the presence (A) and absence of CaM (B) and of NCS-1 (C), showing the glycine amide resonance, and (D) tryptophan $N^{\varepsilon}H$ resonances. (A) is the full ^{15}N-^{1}H spectrum; expanded regions show resonances from only glycine amide (B, C) and tryptophan indole (E) groups Amino acid sequence of PQ1909-2035 with glycine and tryptophan residues highlighted in bold blue. The likely CaM and NCS-1 binding region is indicated *(15).*

FIGURE 4 - *Binding of the PQIQ peptide to NCS-1 monitored using tryptophan fluorescence*. Changes in tryptophan fluorescence following sequential additions of PQIQ peptide to the final concentrations indicated. Recombinant NCS-1 at a concentration of 1μM in a buffer (50mM Tris (pH 7.5), 50mM NaCl, 5mM $CaCl_2$) was titrated with PQIQ at 50μM—1mM in the same buffer conditions. The data were fitted using a logistic equation and non-linear curve fitting.

FIGURE 5 - *^{1}H TOCSY and HSQC spectra showing PQIQ-NCS-1 interactions* (A) TOCSY spectrum of PQIQ peptide delineates NCS-1 binding region. Line-broadening was observed for selected resonances in the presence of a two-fold excess of NCS-1. Line-broadened resolved resonances from Y4, A7, A8, I11 and R16 are highlighted; aromatic resonances (left panel), aliphatic resonances (middle and right panels). (B) ^{1}H-^{15}N HSQC spectra of ^{15}N NCS-1 (0.8mM, black) in the presence of PQIQ (final concentration of 0.4mM, red) in 50mM Tris buffer (pH 6.5), 50mM NaCl, 5mM $CaCl_2$, 300K.

FIGURE 6 – *Expression of NCS-1 and PQ in HeLa cells*. A) HeLa cells were co-transfected with NCS-1-mCherry (red) and EYFP (green) or (green) and mCherry (red) or, B) NCS-1-mCherry (red) and ^{myr}PQ-YFP (green). Regions of co-localisation appear yellow in overlay images. Scale bars = 10μm. C) Quantification of data from A & B. Cells were counted and scored for the presence of puncta (three independent experiments from each control condition

(NCS-1-mCh + EYFP and ^{myr}PQ-YFP + mCherry, (A)) or four independent experiments from ((B) NCS-1-mCh + ^{myr}PQ-YFP). The total number of cells counted for all experiments and for each condition is shown above the corresponding bar on the histogram. All data are plotted as mean ± SEM.

Supplementary material

Table 1 – Average densitometry data for 3 independent NCS-1/GST PQ binding assays described in Figure 1A. Maximal binding (NCS-1 bound to GST-PQ in the presence of calcium for all experiments) was set to 100% binding. Minimum binding for each assay (NCS-1 bound to either GST-CBD or $GST^{IM\rightarrow EE}$ in the absence of calcium depending on the experiment) was set to 0% binding. All other data were normalised in this range.

Condition	Average NCS-1 bound (%)	± % (SEM, n=3)
GST-PQ + Ca^{2+}	100	-
GST-PQ – Ca^{2+}	31.2	3.7
GST-CBD + Ca^{2+}	20.3	10.2
GST-CBD – Ca^{2+}	4.9	4.9
$GST^{IM\rightarrow EE}$ + Ca^{2+}	10.3	3.9
$GST^{IM\rightarrow EE}$ - Ca^{2+}	2.8	2.0

Figure 1

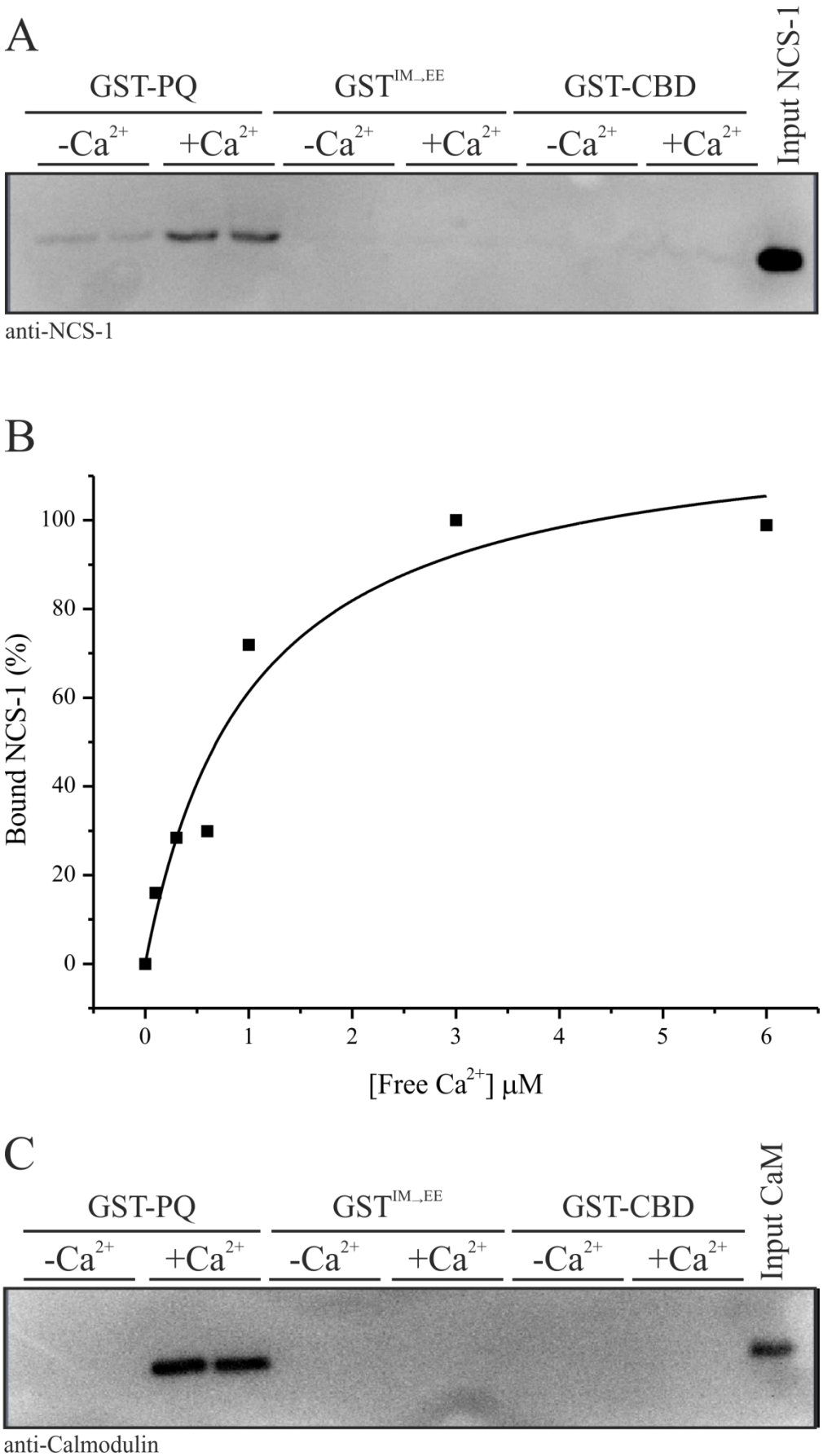
A
GST-PQ
GST$^{IM\rightarrow EE}$
GST-CBD
-Ca^{2+}
+Ca^{2+}
-Ca^{2+}
+Ca^{2+}
-Ca^{2+}
+Ca^{2+}
Input NCS-1
anti-NCS-1
B
Bound NCS-1 (%)
0
20
40
60
80
100
0
1
2
3
4
5
6
[Free Ca^{2+}] μM
C
GST-PQ
GST$^{IM\rightarrow EE}$
GST-CBD
-Ca^{2+}
+Ca^{2+}
-Ca^{2+}
+Ca^{2+}
-Ca^{2+}
+Ca^{2+}
Input CaM
anti-Calmodulin

Figure 2

A

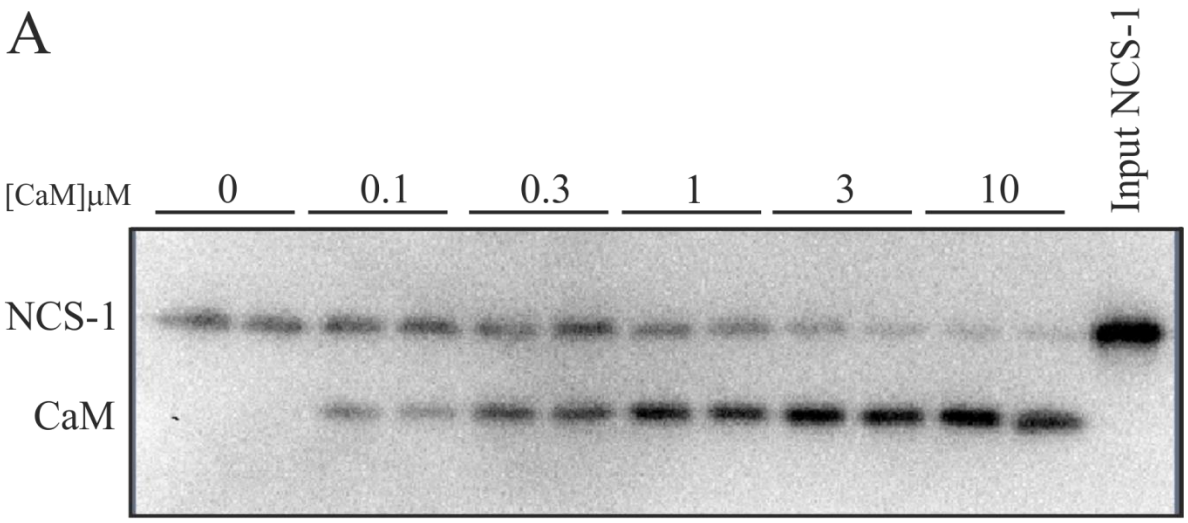
[CaM]μM
0
0.1
0.3
1
3
10
Input NCS-1
NCS-1
CaM

B

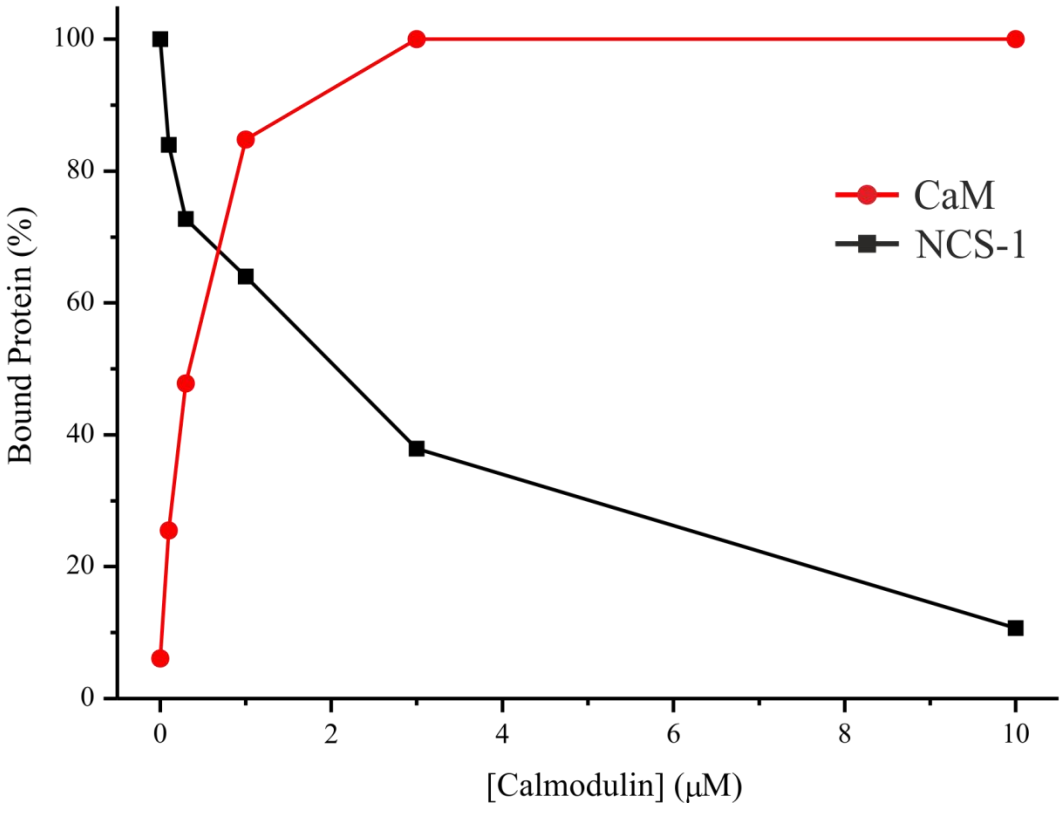
Bound Protein (%)
100
80
60
40
20
0
0
2
4
6
8
10
[Calmodulin] (μM)
CaM
NCS-1

Figure 3

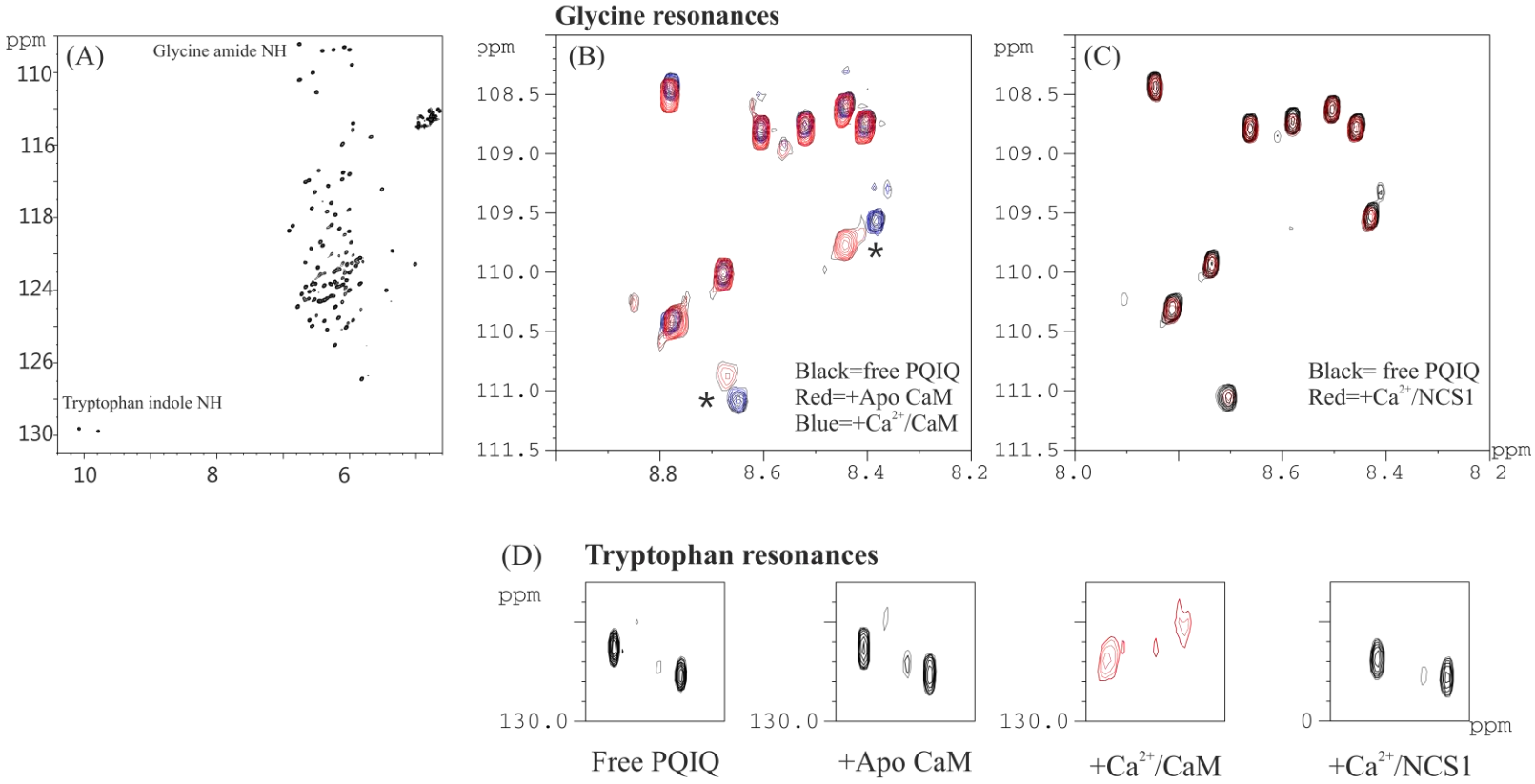

(E)

NCS-1 and Calmodulin/Ca^{2+} binding

^{1909}AAMMIMEYYRQSKAKKLQAMREEQNRTPLMFQRMEPPSPTQ ^{1950}EGGPSQNALPSTQLDP
GGGLMAQESSMKESPSWVTQRAQEMFQKTGTWSPERGPPIDMPNSQPNSQSVEMREMGTDGYSDS^{2035}

Figure 4

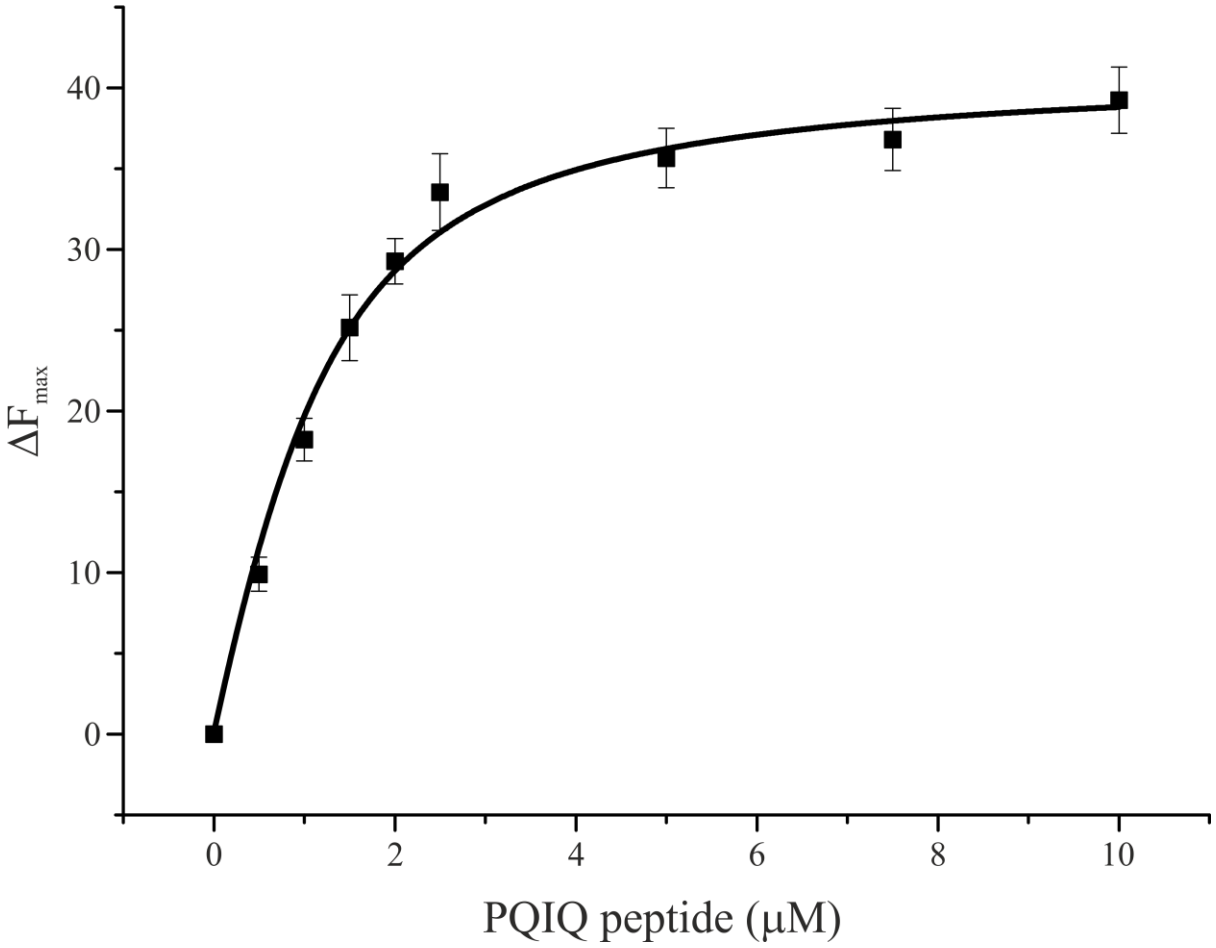

Figure 5

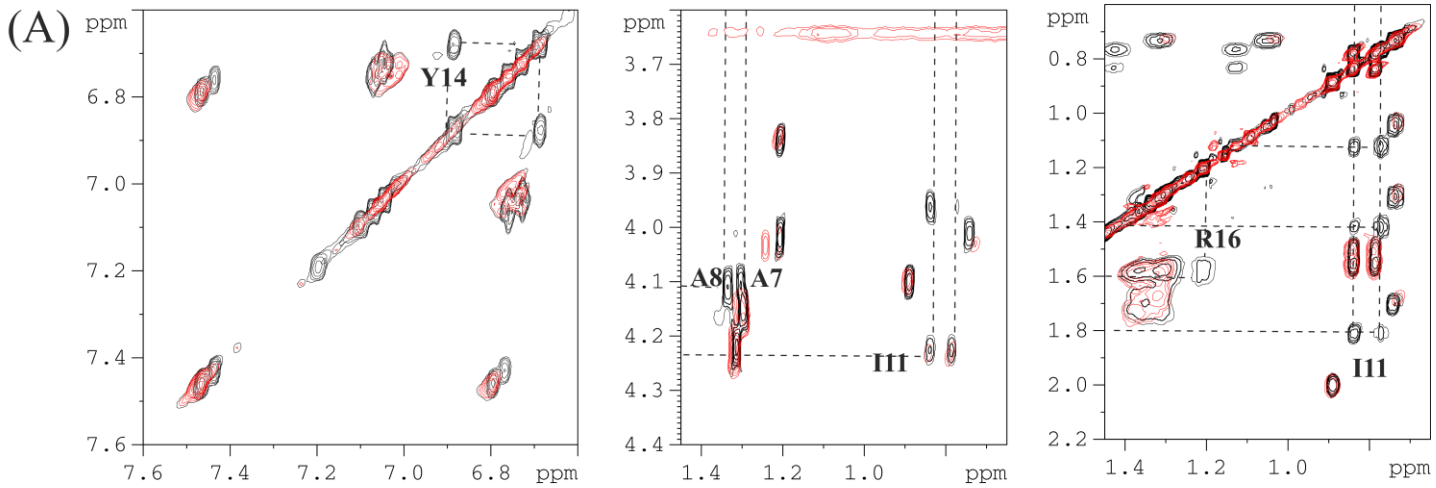

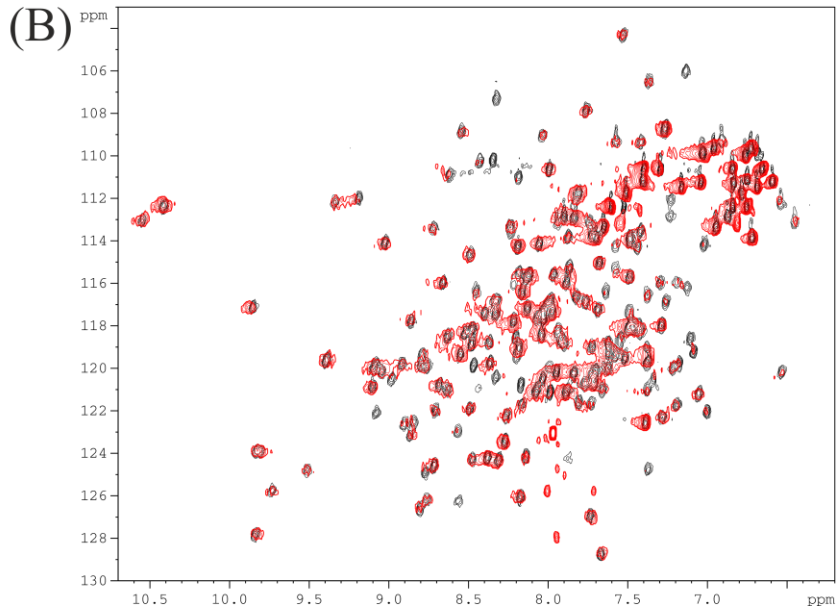

Figure 6

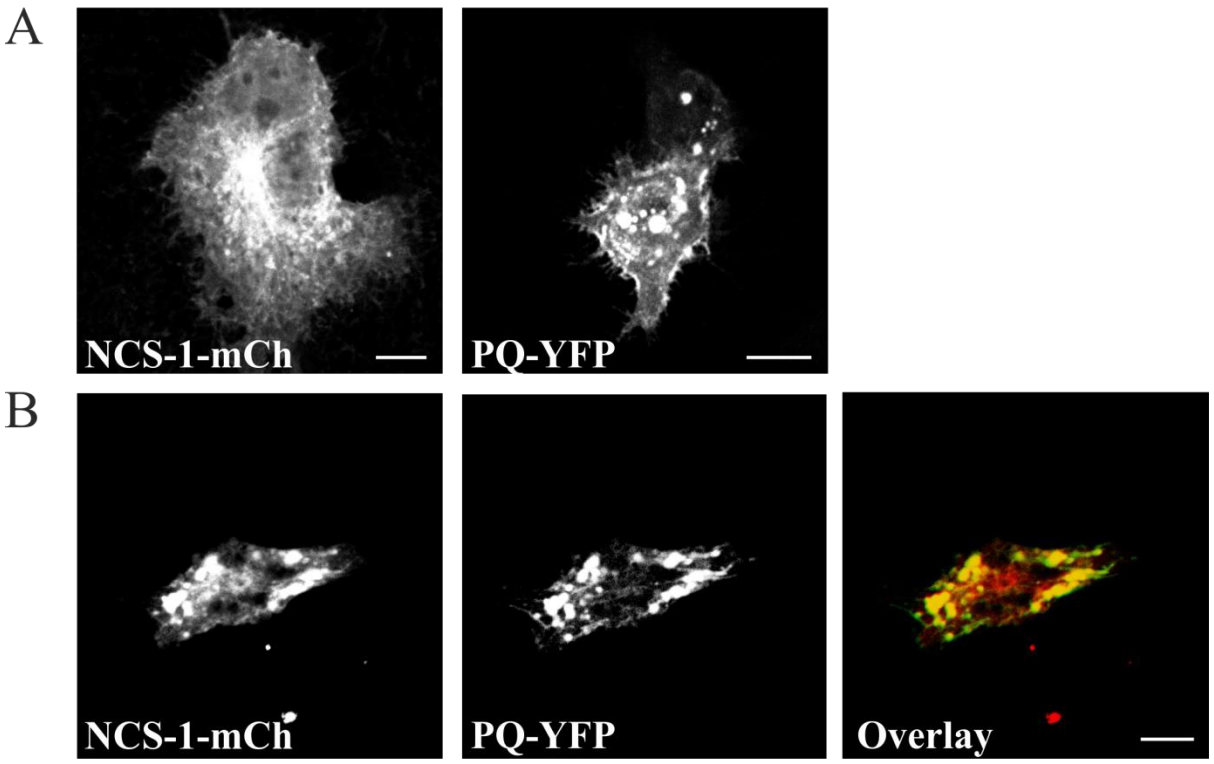
A
NCS-1-mCh
PQ-YFP
B
NCS-1-mCh
PQ-YFP
Overlay

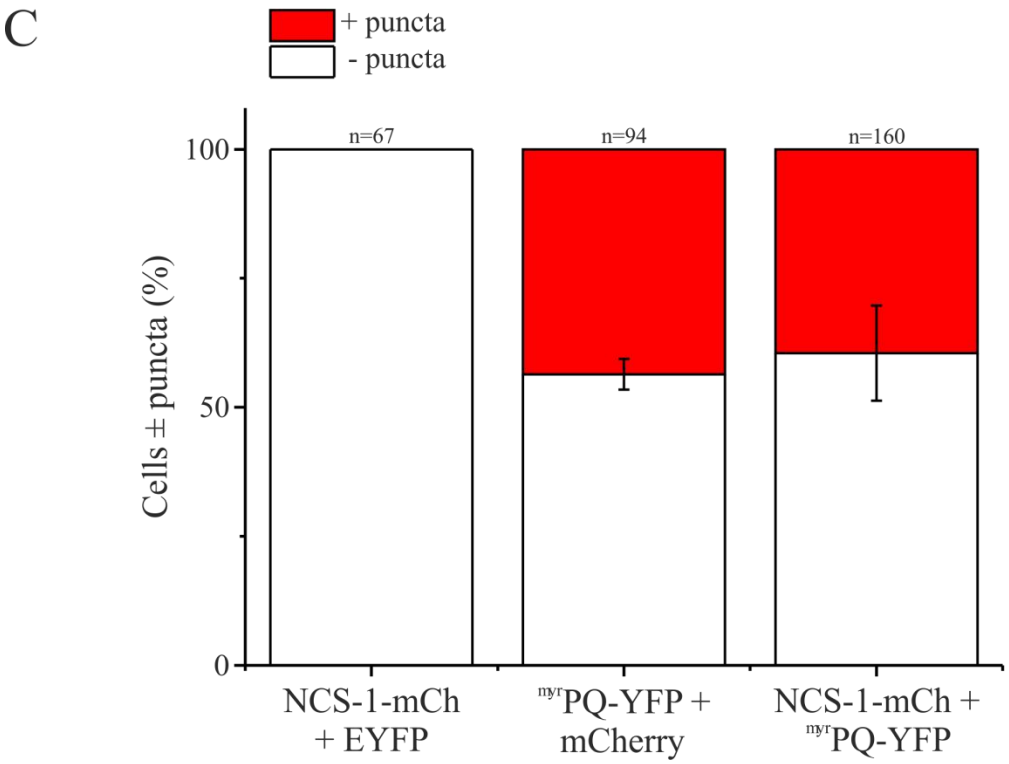
C
+ puncta
- puncta
n=67
n=94
n=160
100
50
0
Cells ± puncta (%)
NCS-1-mCh + EYFP
myrPQ-YFP + mCherry
NCS-1-mCh + myrPQ-YFP